Materials Advances

ROYAL SOCIETY OF CHEMISTRY

PAPER

View Article Online
View Journal | View Issue

Cite this: *Mater. Adv.*, 2025, 6, 5991

Beeswax-modified super hydrophobic acrylonitrile butadiene styrene/polyurethane electrospun membrane for effective oil–water separation†

Muhammed Shabeer, Maria Mathew, Manaf Olongal and Sujith Athiyanathil *

In this work, we report the fabrication and performance of a superhydrophobic acrylonitrile butadiene styrene (ABS)/polyurethane (PU) electrospun membrane modified with beeswax (BW) for oil–water separation. The poor spinnability and mechanical strength of the electrospun ABS membrane were modified by blending it with PU, which has excellent mechanical strength. To the ABS/PU blend electrospun membrane, pure BW was loaded in four different compositions (3–10%). The blend membrane containing 5 wt% beeswax (ABS/PU–5BW) exhibited superhydrophobicity with a water contact angle of 150 ± 4° and an oil absorption capacity of 20.5–23.5 g g^{-1} with an average recovery of 87.55–81.64% in different oils. Moreover, it showed significant potential for gravity-driven oil/water separation, with a separation efficiency of 98.14%. The ABS/PU–5BW membrane has significant reusability efficiency even after 12 cycles of oil absorption and gravity-driven oil–water separation. The optimized membrane exhibited significant thermal and mechanical stability, as well as durability under extreme conditions, such as UV exposure and varying pH levels. Thus, our study developed a novel polymer-blend electrospun membrane modified with beeswax with potential applications in industrial oily wastewater treatment and oil spill remediation.

Received 5th May 2025,
Accepted 14th July 2025

DOI: 10.1039/d5ma00438a

rsc.li/materials-advances

1. Introduction

The rapid development of technology and industrialization exposes us to various forms of organic and inorganic water pollution.[1] Maritime shipping, crude oil refineries, metallurgical processes, and the chemical and textile industries produce significant amounts of oily wastewater as a byproduct.[2,3] The existence of organic pollutants and pathogenic germs in drinking water causes significant health hazards.[4] Approximately 140 000 liters of oil are spilled into the oceans daily.[5] The incorporation of water-insoluble solvents such as chloroform, methylene chloride, benzene, and cyclohexane into water sources also leads to wastewater contamination.[6] This oil-contaminated wastewater contributes to environmental degradation and significant financial losses due to the depletion of hydrocarbons as an energy resource.[7] To address this growing environmental challenge, it is essential to develop efficient materials and techniques for oil–water separation. This issue has been recognized as a global concern recently.[8] Nowadays, there are many conventional methods to overcome this challenge, including flotation, coagulation, biological treatment, and membrane separation technology.[9,10]

Membrane-based separation is one of the efficient methods for oil/water separation.[3] It exceeds other methods in terms of simple operation, energy conservation, normal temperature operation, low cost, and no waste.[11,12] Even oil drops smaller than 10 micrometres can be separated using a membrane.[13] Due to the high mechanical strength, uniform structure, simple synthetic method, and high selectivity, polymer membranes currently dominate the research field.[14] Polymeric membranes have been utilized in several applications, such as the extraction of heavy metals and dyes, oil–water separation, antifouling, and antibacterial functions.[15] Commonly used polymers for water filtration are polyurethane (PU), acrylonitrile butadiene styrene (ABS), polyacrylonitrile (PAN), polyvinylidene fluoride (PVDF), and cellulose acetate (CA).[14,16] Researchers have recently discovered polymer membranes with antibacterial properties, which could be a new step in oil/water purification.[17] Water purification can be achieved by many membrane techniques, including ultrafiltration, nanofiltration, and reverse osmosis. However, these methods are insufficient for the complete separation of minute oil droplets, and there is a considerable risk of membrane damage due to oil penetration into the membrane's pores.[18]

Material Research Laboratory, Department of Chemistry, National Institute of Technology Calicut, Calicut-673601, Kerala, India.
E-mail: athiyanathil.sujith@gmail.com, sujith@nitc.ac.in; Tel: +91 9846475675

† Electronic supplementary information (ESI) available. See DOI: https://doi.org/10.1039/d5ma00438a

This challenge can be addressed by using hydrophobic membranes.[19] Hydrophobic materials can selectively absorb oil from an oil/water mixture with enormous amounts of oil, with high flux and efficiency.[20,21] Membranes are classified as hydrophobic or hydrophilic depending on the contact angle that water makes on the membrane surface. If the contact angle is less than 90°, it is hydrophilic and an angle greater than 150° makes the surface superhydrophobic, which promises an excellent property for oil–water separation.[22] Superhydrophobic membranes can self-regulate surface energy, act as a rough surface, and remain stable for longer periods.[23] Recently, inorganic superhydrophobic materials have been identified as interesting possibilities for practical applications, including self-cleaning, anti-icing, corrosion resistance, and oil–water separation.[24,25] For example, rare earth oxides like cerium oxide have exhibited exceptional performance in properties with high hardness, high thermal stability, and hydrophobicity.[26] Various methods are available for fabricating hydrophobic membranes, including surface coating, solvent casting, and electrospinning techniques.[27] Superhydrophobic membranes fabricated using the electrospinning technique possess numerous advantages, including nanoscale rough surfaces, higher porosity, extensive surface area to volume ratios, and enhanced permeability.[28,29] Electrospinning is a highly versatile technique that enables the production of ultrathin fibres under the influence of a high voltage electric field.[30] Owing to their nanoscale dimensions, electrospun membranes exhibit superior properties over other fabrication techniques. In this study, a simple blending method that integrates natural beeswax lipids with ABS and PU was utilised to fabricate a superhydrophobic membrane for efficient oil–water separation. Among various polymer blends, ABS/PU was distinguished as an optimal choice for developing superhydrophobic oil/water separation membranes because of its excellent mechanical and thermal stability as well as low water absorption.[31]

In this study, we report the fabrication and performance of a superhydrophobic acrylonitrile butadiene styrene (ABS)/polyurethane (PU) electrospun membrane modified with beeswax (BW) for oil–water separation. The electrospinning technique enables the production of nanoscale-sized, porous, high-surface area and high-strength membranes.[32] ABS is a hydrophobic membrane with low mechanical strength and poor spinnability, while PU has high mechanical strength with low hydrophobicity. The poor spinnability and mechanical strength of the electrospun ABS membrane was modified by blending with 10% to 30% of PU in tetrahydrofuran (THF) as the primary solvent and *N*,*N*-dimethylformamide (DMF) as a secondary solvent. An ABS/PU membrane with a 7 : 3 (THF : DMF) solvent ratio was selected as the optimized composition. Pure BW was incorporated into 7 : 3 ABS/PU membrane at varying concentrations, and the optimal blend was identified as the membrane containing 5 wt% beeswax (ABS/PU–5BW). Among natural waxes, such as beeswax (BW), candelilla wax (CL), and carnauba wax (CB), BW shows significant application potential due to its non-toxicity, thermal and mechanical durability, and enhanced hydrophobicity. Beeswax offers superior sustainability and binds effectively to polymer surfaces without requiring any chemical treatments or binders.[33] Thus, the ABS/PU–5BW electrospun membrane exhibited a superhydrophobic behaviour, highlighting its potential for effective oil–water separation applications.

2. Experimental

2.1 Materials

TECOFLEX™ EG-85A grade thermoplastic polyurethane (TPU, $M_w \approx 120\,604$ g mol^{-1}) was purchased from Lubrizol Advanced Materials, Massachusetts, USA. ABS pellets from Ghaed Bassir Petrochemical Co. of Iran (1.04 g cm^{-3} density, 7.6 g/10 min IF). Beeswax (BW) was collected from local areas (Kerala, India). Dimethylformamide (DMF) and tetrahydrofuran (THF) were purchased from Avra Chemicals, India. Oils such as coconut oil and diesel were collected from the local market of Calicut, India.

Each experiment was performed in triplicate using independently fabricated membranes to ensure consistency. The shown data points represent the average values obtained from these experiments. The variability of the data is shown by vertical error bars, calculated using the sample standard deviation in Microsoft Excel. This method provides a statistically valid representation of the experiment's results.

2.2 Preparation of the ABS/PU–BW membrane

The polymer solution for electrospinning was made by dissolving 1.4 g of ABS (70 wt%) and 0.6 g of PU (30 wt%) in a 7 : 3 (v/v) THF : DMF solvent system by vigorous stirring for 12 h. Pure BW was then added to the solution with constant stirring. Six distinct solutions were prepared with varying the beeswax concentrations from 0 to 10 wt%. The pristine ABS/PU–BW solution was subsequently introduced into a 10 mL syringe fitted with a needle possessing an internal diameter of 0.2 mm, and the solution was dispensed at a regulated flow rate of 3 mL h^{-1}. The needle was linked to a voltage of 18 kV, and the spun fibres were collected on a rotating collector situated 15 cm away from the needle tip. The collected fibers were kept in a hot air oven at 40 °C to eliminate residual solvent.

2.3 Characterization

The morphological characteristics of the electrospun nanofibrous membranes have been studied using field emission scanning electron microscopy (FE-SEM, Zeiss Sigma 300) at an accelerating voltage of 18 kV and confirmed the accumulation of BW on the fibre surface. The mean fibre diameter was analysed by using Image J software by randomly choosing 50 fibres from each membrane. The infrared spectra of the electrospun membranes were acquired by using a Fourier transform infrared spectrometer (PerkinElmer Spectrum™ 2) in ATR-FTIR mode. The reported range for the scans was 4000–500 cm^{-1}. X-ray diffraction patterns of the membranes were obtained using a PANalytical X'Pert^3 powder X-ray diffractometer with a Cu Kα radiation source. The mechanical characteristics of the electrospun membranes of dimensions 0.5 × 5 cm were analysed using a universal testing machine (Schimadzu Autograph, AG-Plus series) with an applied load of 10 N. The thermal properties of

the membranes were analysed by a thermogravimetric analyser (TGA, TA Instruments, Q50) by heating the samples from 30 °C to 700 °C at a rate of 10 °C min^{-1}. The hydrophobicity of the membrane was characterised by measuring the water contact angle with a GBX Digidrop goniometer. The water contact angle was calculated using the sessile drop method and obtained with a software program.

2.4 Oil sorption experiments

The oil absorption capacity of the ABS/PU–BW electrospun membranes was assessed by placing a 2 × 2 cm piece of membrane on the surface of oil in a Petri dish. All the experiments were carried out at room temperature. The absorption capacity of the material was assessed using petroleum-based oil and vegetable oil across five distinct membranes (Table 1). Each membrane was allowed to absorb the oil for 5 minutes, and the absorbent weight was calculated to evaluate the absorption kinetics. The absorption capacity (α) of the different membranes can be calculated using eqn (1),

$$\alpha = \frac{W_f - W_i}{W_i} \quad (1)$$

where W_i is the weight of the dry membrane and W_f is the total weight of the wet membrane.[34]

2.5 Oil–water separation test

The performance of oil–water separation for the membrane was evaluated using gravity-driven oil–water separation approaches. The electrospun membrane was affixed between two glass tubes with a diameter of 2.5 cm. A 50% (v/v) oil–water mixture was introduced at the top of the tube without applying external pressure. The apparatus was positioned at a 45° angle to facilitate contact between the oil layer and the membrane.[35] Two oil–water combinations were examined: diesel/water and coconut oil/water. The flow was determined by quantifying the volume of oil that passed the membrane in one minute using the following equation (eqn (2))

$$F = \frac{V}{At} \quad (2)$$

where F is the flux of oil in L m^{-2} h^{-1}, V is the separated volume of oil per minute (t), and A is the contact area of the membrane. The membrane's separation efficiency was determined using the equation (eqn (3)),

$$R = \frac{(V_m + V_s)}{V_o} \times 100 \quad (3)$$

where V_o is the initial volume of oil, V_s is the volume of oil after separation, and V_m is the volume of oil adsorbed by the membrane.

2.6 Reusability of the membrane

The absorption capacity of the ABS/PU–BW electrospun membrane was assessed for one minute throughout 12 consecutive cycles to evaluate the membrane's reusability. After each absorption cycle, the oil was extracted utilising absorbent paper and subsequently rinsed with ethanol. The oil recovery percentage (R) was determined using the following equation (eqn (4)),

$$R = \frac{W_r}{(W_e - W_o)} \times 100 \quad (4)$$

where W_r is the weight of collected oil from the membrane, W_o is the dry weight of the membrane, and W_e is the weight of the membrane after 1 min absorption.

2.7 Durability tests

The ABS/PU–BW membranes were subjected to UV lamp exposure at a distance of 20 cm for several time intervals to assess their UV resistance. The UV exposure chamber was maintained at a constant temperature of 27 °C with a relative humidity of 55%. After exposure, the samples were examined for water contact angle. To monitor the stability under acidic, basic, and neutral conditions, a droplet of water, 1 M NaOH and 1 M HCl were added to the optimised membrane, and the contact angle was analysed.

3. Results and discussion

3.1 Morphology of the electrospun ABS/PU–BW nanofibrous membranes

The SEM morphologies of the ABS/PU samples with varying concentrations of BW are shown in Fig. 1. SEM images indicate the formation of randomly aligned three-dimensional cylindrical nonwoven fibres with an average fibre diameter between 4.39 μm to 1.87 μm. The bare ABS/PU has an average fibre diameter of 4.3 ± 1.42 μm. A large reduction in the average fibre diameter was seen with an increase in beeswax

Table 1 The description of the samples with sample codes

Sample code	Sample description
ABS/PU	70% ABS/30% PU
ABS/PU–BW3	70% ABS/30% PU + 3% BW
ABS/PU–BW5	70% ABS/30% PU + 5% BW
ABS/PU–BW7	70% ABS/30% PU + 7% BW
ABS/PU–BW10	70% ABS/30% PU + 10% BW

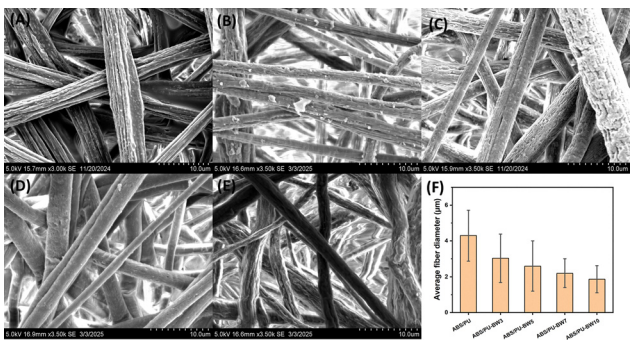

Fig. 1 SEM images of the electrospun ABS/PU samples at different beeswax concentrations. (A) ABS/PU, (B) ABS/PU–BW3, (C) ABS/PU–BW5, (D) ABS/PU–BW7, (E) ABS/PU–BW10, and (F) average fibre diameter of the ABS/PU samples at different beeswax concentrations.

concentration (Fig. 1F). The membrane containing 3 wt% BW has a fibre diameter of 3.03 ± 1.35 μm, while the 10 wt% BW shows the smallest fibre diameter of 1.87 ± 0.76 μm. The significant reduction in average fibre diameter results from the exceptional dispersion of the two hydrophobic matrices. ABS and PU are hydrophobic polymers with excellent thermal properties and electrospinnability[36,37] while BW is a naturally occurring lipid showing prominent hydrophobic characteristics. The main reason for the decrease in average fibre diameter upon the addition of BW is attributable to fluctuations in the viscosity of the spinning dope. A notable decrease in the viscosity of the electrospun solution occurs simultaneously with the gradual rise in BW concentration inside the ABS/PU solutions. This effect arises from the reduced molecular weight of BW in comparison to ABS and PU. In less viscous solutions, the polymer chains are properly segregated and do not overlap, leading to a greater tendency for the creation of electrospun fibres with a decreased diameter.[38] The reduced fibre diameter and rough surface reported in BW loaded ABS/PU membranes indicated an improvement in hydrophobic characteristics.

Fig. 2A and B illustrate the porosity and mean pore radius of various ABS/PU electrospun membranes with different concentrations of beeswax (BW), which significantly influences their surface properties for oil/water separation. Among the samples, ABS/PU–BW5 exhibits the highest porosity (~87%) and the largest mean pore radius (~28 μm), indicating an open and well-connected pore structure that favors efficient oil transport and separation. In contrast, membranes with 3%, 7%, and 10% beeswax show lower porosity and significantly smaller pore sizes (~9–10 μm), and the bare ABS/PU membrane has moderate values for both parameters.

3.2 IR analysis

Fig. 3A illustrates the transmission spectra of pure ABS, PU, and ABS/PU electrospun membranes with different concentrations of beeswax in the 500–4000 cm^{-1} regions. The characteristic absorption band of ABS that appeared at 2930 cm^{-1}, corresponds to the aliphatic C–H stretching mode, and the peaks at 1455 cm^{-1} and 700 cm^{-1} were due to C–H bending vibration and out-of-plane bending vibrations of C–H bonds in the aromatic rings (benzene rings). PU exhibited peaks at 2930 cm^{-1} and 2856 cm^{-1} corresponding to symmetric and asymmetric stretching of the C–H bond. The peaks at 1690 cm^{-1}, 1455 cm^{-1} and 1100 cm^{-1} were due to C═O stretching vibration of the carbamate group

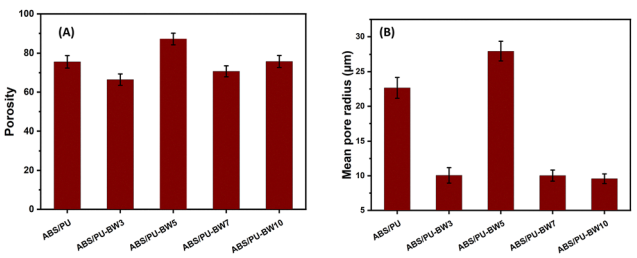

Fig. 2 Effect of BW concentration on (A) porosity and (B) mean pore radius of ABS/PU electrospun membranes.

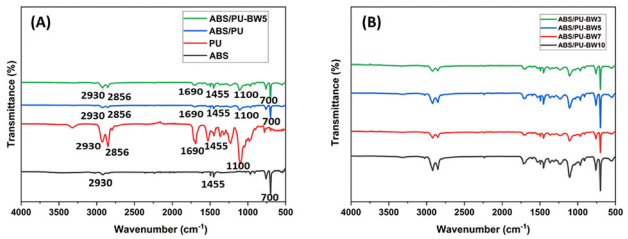

Fig. 3 IR spectra of (A) ABS, PU, ABS/PU and ABS/PU–BW5, and (B) IR spectra, and increment of the C–H stretching peak with the increase in beeswax concentration.

(–NH–COO–), $–CH_2$ bending vibrations, and C–O–C stretching vibrations from the urethane backbone, respectively. The IR spectra of ABS/PU–BW5 showed all characteristic peaks of ABS and PU (Fig. 3A). Fig. 3B illustrates the increase in the intensity of the C–H stretching peak at 2856 cm^{-1} with an increase in beeswax concentration in ABS/PU, due to the higher amount of C–H bonds provided by the beeswax component, and hence increasing the quantity of beeswax elevates the concentration of aliphatic C–H bonds.

3.3 XRD analysis

The XRD spectra of the ABS/PU and ABS/PU–BW electrospun membranes are shown in Fig. 4. Electrospun ABS/PU exhibits one sharp peak at 12.74° and one broad peak at 20.8° with a percentage crystallinity of 46.36% associated with the (110) and (200) planes.[39] Hence, bare ABS/PU is semi-crystalline in nature. The presence of a broad peak along with sharp peaks indicates a semicrystalline material, consisting of both crystalline and amorphous phases.[40] The ABS/PU–BW exhibits a single broad peak at 19.5°. The addition of beeswax to the polymer membranes results in the disappearance of the sharp peak and the appearance of a larger peak, indicating that beeswax enhances the amorphous characteristics of the polymer membrane. A gradual increase in the broadness of the peak was observed from bare ABS/PU to the ABS/PU–BW10 electrospun fibre. The incorporation of beeswax improves the amorphous characteristics of the ABS/PU membrane,

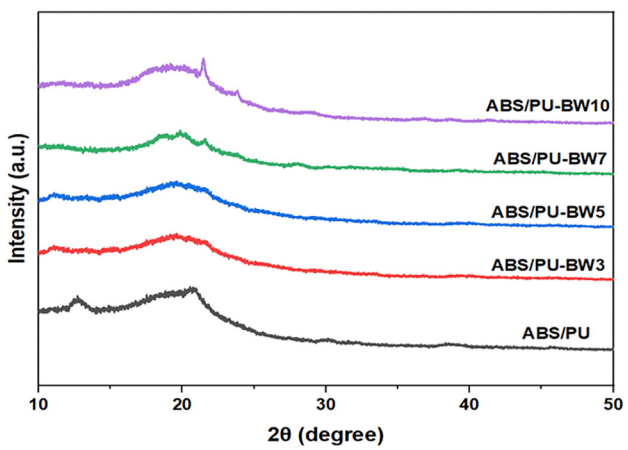

Fig. 4 X-Ray diffraction of the ABS/PU and ABS/PU–BW electrospun membranes.

enhancing surface roughness and hydrophobicity. This structural modification enhances water repellence and oil selectivity, making the membrane highly efficient for oil–water separation.

3.4 Tensile properties

High tensile strength and elongation, along with excellent shape recovery and retention, are important parameters needed for an effective and reusable oil-absorbent membrane. Fig. 5A illustrates the percentage of elongation curves for various ABS/PU–BW electrospun membranes. Initially, ABS exhibits a lower percentage elongation of 6 ± 0.6, whereas PU shows a significantly higher elongation of 80 ± 3. The high elongation of PU is due to its flexible, amorphous structure containing soft segments that facilitate easier deformation of the polymer.[41] ABS, characterized by its increased crystallinity and rigidity, has reduced elongation and is more prone to fracture under stress.[42] The incorporation of BW into the ABS/PU electrospun membrane enhances the % elongation from 36 ± 2.5 to 42 ± 2.9, 50 ± 2.8, and 51 ± 2.7 for ABS/PU–BW3, ABS/PU–BW5, and ABS/PU–BW7 membranes, respectively. The rise in percentage elongation with the increase of BW concentration indicates that the incorporation of BW has conferred significant enhancement of membrane flexibility and viscoelastic characteristics. It is due to the plasticizer effect of BW, which enhances chain mobility, alters phase morphology, and decreases crystallinity. Also, BW acts as a lubricant among high molecular weight ABS/PU molecules, enhancing the percentage elongation.[43] However, ABS/PU–BW10 has a reduced % elongation of 40 ± 2.5 due to the excessive beeswax, which might result in improper dispersion, excessive softening, disruption of polymer chain interactions, and increased brittleness. These factors collectively decrease the % elongation.[44]

Fig. 5B shows the tensile strength of the resultant membranes. The integration of BW into the ABS/PU membrane leads to a notable reduction in tensile strength from 2.3 ± 0.2 MPa to 1.6 ± 0.2 MPa. However, a further increase in the concentration of BW, from 3% to 10%, yields only a negligible decrease in the tensile strength of the electrospun membranes. BW has features of low molecular weight lipids, filling the interstices of high molecular weight polymer chains and acting as a lubricant. The lipid content of BW diminishes intermolecular interactions among the ABS/PU long chains, leading to a drop in tensile strength. The optimized ABS/PU–BW system exhibits excellent mechanical properties, including high tensile strength and percentage elongation. The incorporation of BW enhances elongation by lowering the crystallinity and increasing the polymer chain mobility. This improvement is comparable to various inorganic systems, such as FAS-SiO_2@PDA/PU, which demonstrate exceptional mechanical durability under dynamic and harsh conditions like high-pressure abrasion and repeated compression.[45]

Fig. 5C shows that the Young's modulus of ABS/PU films decreased with beeswax (BW) content up to 7%, indicating enhanced softness and flexibility. At 10% BW, the modulus increased, suggesting structural changes that improved stiffness. Fig. 5D presents stress–strain curves of various ABS/PU electrospun membranes. All samples initially exhibited nonlinear elastic behaviour, followed by a stable region with increasing elongation under nearly constant stress. Strain increased with BW content, with ABS/PU breaking at 30% strain and ABS/PU–BW7 at 80%, reflecting improved flexibility and viscoelasticity due to the lubricating effect of natural lipids in BW. However, excess BW (10%) caused brittleness, reducing strain to 30%. An optimized ABS/PU–BW membrane with high elasticity was thus developed, making it a strong candidate for oil/water separation.

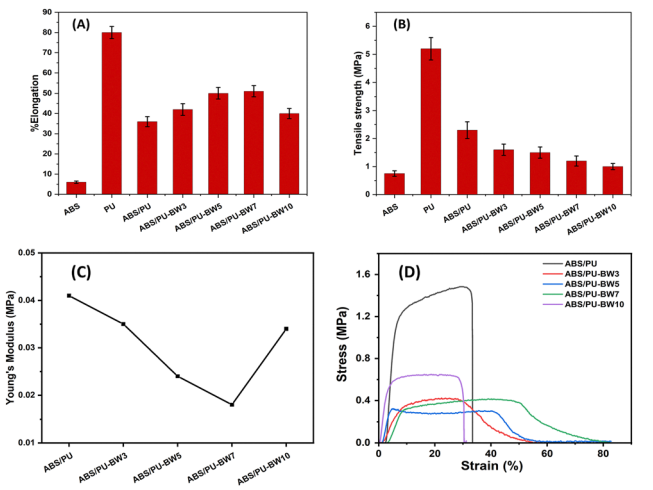

Fig. 5 (A) % elongation diagram of ABS/PU membranes with different beeswax. (B) Variation in tensile strength of ABS/PU membranes with different beeswax concentration. (C) Young's modulus of ABS/PU membranes with varying BW concentration and (D) stress–strain curves of ABS/PU and ABS/PU–BW composite membranes.

3.5 TGA analysis

TGA analysis was conducted to assess the thermal stability of ABS/PU–BW electrospun membranes. Fig. 6A shows the TGA curves of BW and electrospun ABS/PU–BW membranes with different concentrations of BW. The onset temperatures (T_o), initial degradation temperature (T_1 max), temperature corresponding to 50% weight loss (T_{50}), and temperature for maximal degradation rate (T_2 max) were evaluated and presented in Table 2. Incorporating beeswax (BW) into ABS/PU electrospun composite membranes enhances the thermal stability of the polymer membranes, as indicated by increases in T_1 max and T_2 max. This improvement is observed with BW concentrations

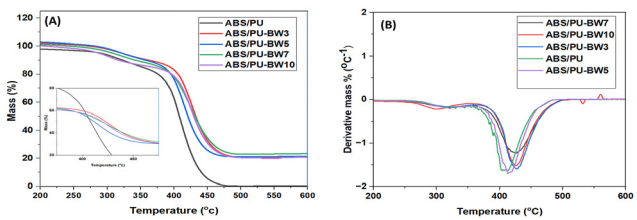

Fig. 6 A) TGA curves of ABS/PU and ABS/PU–BW composite membranes, (B) DTG curves of ABS/PU and ABS/PU–BW composite membranes.

Table 2 Characteristic degradation temperatures of electrospun ABS/PU–BW membranes

Sample	T_o (°C)	T_1 max (°C)	T_{50} (°C)	T_2 max (°C)
ABS/PU	270	309	402	410
ABS/PU–BW3	280	320	410	420
ABS/PU–BW5	288	326	407	413
ABS/PU–BW7	287	324	418	420
ABS/PU–BW10	269	308	420	418

ranging from 3% to 7%. However, when the BW concentration exceeds 7%, T_o and T_1 max begin to slightly decrease. This decline is attributed to the excessive accumulation of BW on the membrane surface, which results in non-uniform surface roughness, a plasticization effect, and phase separation, all of which can negatively impact the membrane's thermal stability.

Fig. 6B provides information about the first derivative of the TGA thermogram (DTG), which analyses the effect of BW concentration on degradation temperature. The DTG curve illustrates that the T_1 max and T_2 max of the optimum BW-coated electrospun composite membranes are higher than those of the bare ABS/PU electrospun membrane, indicating that the composites have improved thermal stability. Due to the presence of the BW, a significant barrier effect is created that restricts the diffusion of degradation products from the polymer bulk to the gas phase. Additionally, the fibrous morphology of the membrane serves as a protective network, minimising the release of decomposition gases from the polymeric matrix.[46]

3.6 Water contact angle

Pure ABS and PU are hydrophobic polymers, showing lower surface energy of 40 mJ m^{-2} and 45 mJ m^{-2}, respectively. Consequently, both electrospun membranes exhibited water contact angles (WCA) of 138 ± 2.5° and 110 ± 2°, with water droplets remaining on the surface of the samples for a longer time. The incorporation of BW in ABS/PU has shown a significant increase in WCA towards superhydrophobicity, as shown in Fig. 7. Wettability was dependent on surface roughness, surface free energy, and chemical composition of the membranes. With increasing concentration of BW in ABS/PU, the water contact angle rises progressively due to the reduction in surface free energy and the enhancement of surface roughness.[47,48] As a result, the BW coated electrospun membrane shows a remarkably higher WCA than the bare ABS/PU electrospun membranes.

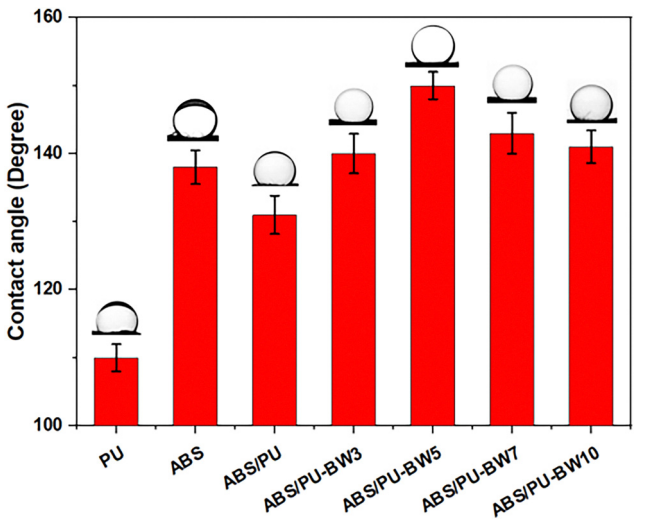

Fig. 7 Water contact angle of ABS/PU and ABS/PU–BW composite membranes.

The ABS/PU–BW5 membrane exhibited superhydrophobic behaviour with a WCA of 150 ± 2°. As expected from WCA analysis, ABS/PU–BW5 showed excellent oleophilicity and high selective oil sorption capacities from the water surface compared to all other samples. While ABS/PU–BW7 and ABS/PU–BW10 show WCAs of 143 ± 8° and 141 ± 3°, respectively. From 5% of BW drastically decreased in WCA due to the accumulation of excess BW on the polymer surface. This leads to non-uniform surface roughness, plasticization effect, phase separation and surface energy changes, which all can disrupt the polymer structure, leading to a decrease in the water contact angle.[49,50] As a result, ABS/PU–BW5 achieved a superhydrophobic character and is considered an optimised concentration of the beeswax to provide uniform dispersion and prevent defects that facilitate water spreading.

3.7 Oil sorption capacity

The ABS/PU electrospun membranes with varying BW concentrations were evaluated for their oil sorption capacity. The ABS/PU–BW5 membrane exhibited superhydrophobic properties with a WCA of 150 ± 2°. According to WCA studies, ABS/PU–BW5 demonstrated exceptional oleophilicity and significant selective oil sorption capacities from the water surface. Fig. 8A–D depicts the image of selective oil absorption from the water surface. 1 ml of diesel, coloured with methylene red oil dye, was deposited onto a Petri dish filled with water. A rectangular membrane measuring 4 cm^2, composed of ABS/PU–BW5, and possessing a thickness of 0.25 mm was positioned in contact with a floating thin layer of oil on the water surface. The membrane rapidly absorbs the oil while repelling the water, as illustrated in Fig. 7C. Thus, the oil layer was completely removed by membrane sorption, resulting in a fully pure water surface (Fig. 8D).

Fig. 8E illustrates the saturated oil sorption capacity for various ABS/PU–BW membranes. The pure PU electrospun

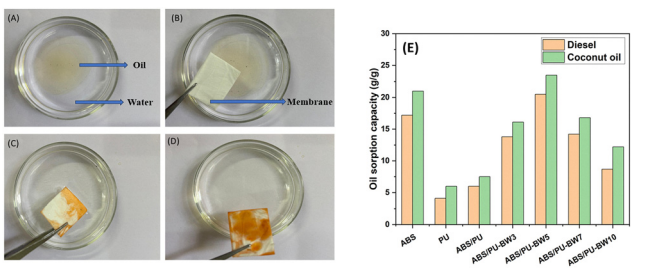

Fig. 8 (A)–(D) Images of selective absorption of diesel from the water surface with ABS/PU–BW5 membranes. (E) Maximum oil absorption capacity of various concentrations of ABS/PU–BW membranes in diesel and coconut oil.

membranes exhibited a minimal oil sorption capacity of 4.1–6 g g^{-1} for different oils, whereas ABS had a greater oil sorption capacity of 17.2–21 g g^{-1}. The ABS/PU electrospun membrane exhibited a minimal saturated oil sorption capacity of 6–7.5 g g^{-1} due to its relatively low hydrophobicity; hence, oil molecules are limited to only the external pores of the membranes without solvation. The incorporation of beeswax in ABS/PU electrospun membranes enhances the oil sorption capacity, with ABS/PU–BW5 achieving a maximum capacity of 20.5–23.5 g g^{-1} for various oils. This phenomenon can be assigned to the increased hydrophobicity, roughness, and porosity of ABS/PU–BW5. ABS/PU–BW7 and ABS/PU–BW10 show absorption in the range of 14.2–16.8 g g^{-1} and 8.7–12.2 g g^{-1}, respectively, indicating that an excess of BW decreases the oil sorption capacity of electrospun membranes due to reduced porosity, increased rigidity, and phase separation, which creates defects in the membrane structure.[51]

3.8 Gravity-driven oil–water separation

The ABS/PU–BW5 membrane exhibits significant potential for gravity-driven oil–water separation due to its superhydrophobic properties. The membrane, unsupported by any other membranes, has been analysed for oil flux. Oil–water mixes were analysed for gravity-driven flux, as shown in Fig. 9A–C. A mixture of water and diesel was poured onto the ABS/PU–W5 membranes placed between two glass tubes. The arrangement was placed at an angle to allow diesel to contact the membrane. Due to the superhydrophobic and superoleophilic properties of ABS/PU–BW5 membranes, diesel rapidly permeated through the membrane and fell into the beaker, while water stayed above the membrane. Throughout this procedure, the light oil layer was in partial contact with the membrane.

Fig. 9D shows the flux of diesel–water and coconut oil–water mixes throughout 12 cycles. Beginning with the sixth cycle, the flow of ABS/PU–BW5 membranes experiences a slight reduction due to the partial degradation of the fibrous shape. The diesel–water mixture showed an average flux of 295.03 L m^{-2} h^{-1}. Similarly, high-viscosity vegetable oils, such as coconut oil, exhibited an average flux of 29.51 L m^{-2} h^{-1}. The oil/water separation efficiency *versus* the number of cycles was analysed by taking the diesel–water and coconut oil–water mixture (Fig. 9E). The ABS/PU–BW5 membrane showed a significant separation efficiency of 98.14% and 93.22%, respectively, even after 12 cycles. These results confirmed that the ABS/PU–BW5 membrane possesses significant efficacy in removing oil contaminants from water.

3.9 Recyclability

The reusability of ABS/PU–BW5 polymer membranes was examined for twelve sorption cycles using various oil–water mixtures, as shown in Fig. 10. After each cycle, the absorbed oil on the electrospun membrane was removed by rinsing with ethanol followed by drying. The average recoveries for diesel and coconut oil are 87.55% and 81.64%, respectively. Following 12 sorption cycles, the ABS/PU–BW5 membrane showed a reduction in sorption efficiency of only 12.45% for diesel and 18.31% for coconut oil. The ABS/PU–BW5 membrane exhibited a water contact angle of 149 ± 2° even after 12 cycles of oil absorption, indicating sustained surface hydrophobicity (Fig. 10C). The observed reusability and enhanced recovery efficiency further indicate the membrane's excellent chemical and mechanical stability in various oil conditions. Theoretically, 1 kg of the membrane may recover about 154 kg of diesel and 208 kg of coconut oil throughout 12 reuse cycles. The results indicate that the membrane modified with BW shows significant potential as a reusable membrane for effective oil/water separation.

3.10 Durability

The durability and stability of oil-absorbent membranes in harsh conditions are essential for their efficient use. The

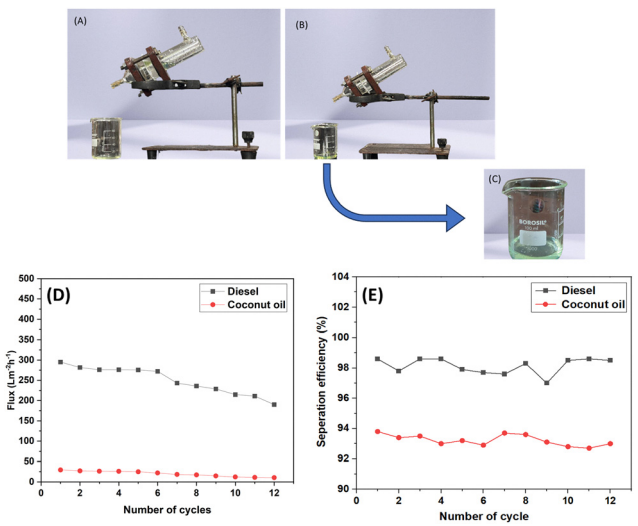

Fig. 9 (A)–(C) Gravity-driven diesel–water separation setup. (D) Changes in diesel–water and coconut oil–water flux with 12 cycles of separation and (E) separation efficiency of diesel and coconut oil at 12 cycles of separation.

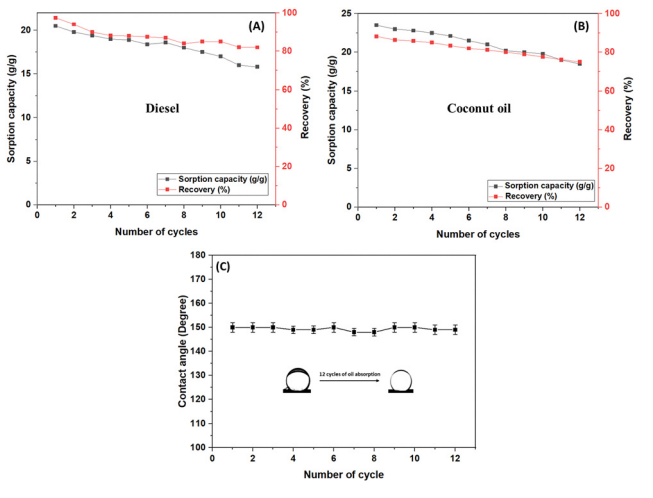

Fig. 10 Reusability and recovery percentage of the ABS/PU–BW5 membranes in (A) diesel, (B) coconut oil and (C) changes in WCA with 12 cycles of separation and WCA images of the ABS/PU–BW5 surface before diesel–water separation and after 12 separation cycles.

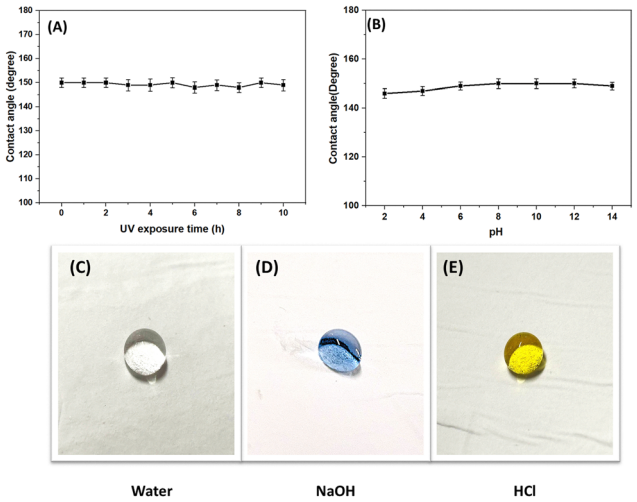

Fig. 11 (A) Contact angles of the ABS/PU–BW5 membrane under different times of UV exposure, (B) under different pH ranges, (C) photographs of a water drop, (D) a 1 M-NaOH drop, and (E) a 1 M-HCl drop.

ABS/PU–BW5 superhydrophobic electrospun membranes were subjected to durability assessments under different periods of UV exposure. Fig. 11A shows the variations in the water contact angle corresponding to various durations of UV exposure. The membrane exhibited remarkable UV resistance after 12 hours of exposure and maintained superhydrophobicity, with average contact angles of 149 ± 2°. Fig. 11B illustrates the contact angle measurements of the ABS/PU–BW5 membrane across a pH range of 2 to 14 in order to check the stability under acidic and basic conditions. The ABS/PU–BW5 membrane showed superhydrophobicity with average contact angles of 148 ± 3° from a pH range of 6–14 even after 12 hours of immersion time. These findings suggest that the ABS/PU–BW5 membrane is well-suited for applications in chemically aggressive environments, such as oil–water separation or anti-fouling coatings.[52] Fig. 11(C)–(E) displays images illustrating the contact angle of the membrane with water droplets, alongside droplets of 1 M NaOH and 1 M HCl. The results indicate that the ABS/PU–BW5 membrane exhibits significant resistance to water corrosion, even in very acidic and basic conditions, implying that ABS/PU–BW5 is an excellent choice for oil–water sorption in demanding environments.

4. Conclusion

In summary, a novel, environment-friendly ABS/PU blended electrospun membrane was synthesised by using the electrospinning technique. The optimised 7 : 3 ABS/PU membrane system was modified with pure BW and shifted from hydrophobic to superhydrophobic behaviour. The resultant membrane with 5 wt% BW concentration exhibited a rough surface morphology and superhydrophobicity with a water contact angle of 150 ± 2°. The membrane exhibited a high oil absorption capacity of 20.5–23.5 g g^{-1} with average recoveries of 87.55–81.64% in different oils. Furthermore, it demonstrated considerable potential for gravity-driven oil–water separation, with a separation efficiency of 98.14% even after 12 cycles. The ABS/PU–5BW membrane exhibited superior thermal stability and good mechanical strength. The improved membrane exhibited significant environmental resilience under extreme conditions, including ultraviolet exposure and varying pH levels. This work examines a new area of superhydrophobic hybrid membranes utilising beeswax as a functional material for selective oil/water separation.

Author contributions

Muhammed Shabeer: conceptualization, methodology – writing original draft. Maria Mathew: review and editing. Manaf Olongal: review and editing. Sujith Athiyanathil: supervision, review and editing.

Conflicts of interest

There are no conflicts of interest to declare.

Data availability

The data that support the findings of this study are available on request from the corresponding author.

Acknowledgements

The authors gratefully acknowledge the financial support provided by the National Institute of Technology Calicut (NITC), India, for this research work.

References

1 X. Xu, Y. Yang, T. Liu and B. Chu, Cost-Effective Polymer-Based Membranes for Drinking Water Purification, *Giant*, 2022, **10**, 100099.
2 O. Manaf, K. Anjana, R. Prasanth, C. R. Reshmi, K. Juraij, P. Rajesh, C. Chingakham, V. Sajith and A. Sujith, ZnO Decorated Anti-Bacterial Electrospun ABS Nanocomposite Membrane for Oil-Water Separation, *Mater. Lett.*, 2019, **256**, 126626.
3 T. E. Oladimeji, M. Oyedemi, M. E. Emetere, O. Agboola, J. B. Adeoye and O. A. Odunlami, Review on the Impact of Heavy Metals from Industrial Wastewater Effluent and Removal Technologies, *Heliyon*, 2024, **10**(23), e40370.
4 L. Lin, H. Yang and X. Xu, Effects of Water Pollution on Human Health and Disease Heterogeneity: A Review, *Front. Environ. Sci.*, 2022, **10**, 880246.
5 R. K. Gupta, G. J. Dunderdale, M. W. England and A. Hozumi, Oil/Water Separation Techniques: A Review of Recent Progresses and Future Directions, *J. Mater. Chem. A*, 2017, **5**(31), 16025–16058.
6 X. Zhang, R. Dai, H. Sun, Y. Zhang, D. Liu, M. Wang, M. Sun and H. Yu, Mandelic Acid-Derived Organogelators: Applications of Their Solid Form in Rapid and Efficient

Remediation of Marine Oil Spills, *Mater. Chem. Front.*, 2019, **4**(1), 222–230.
7 J. Beyer, H. C. Trannum, T. Bakke, P. V. Hodson and T. K. Collier, Environmental Effects of the Deepwater Horizon Oil Spill: A Review, *Mar. Pollut. Bull.*, 2016, **110**(1), 28–51.
8 R. S. Sutar, S. S. Latthe, S. Nagappan, C. S. Ha, K. K. Sadasivuni, S. Liu, R. Xing and A. K. Bhosale, Fabrication of Robust Self-Cleaning Superhydrophobic Coating by Deposition of Polymer Layer on Candle Soot Surface, *J. Appl. Polym. Sci.*, 2021, **138**(9), 49943.
9 L. Yu, M. Han and F. He, A Review of Treating Oily Wastewater, *Arabian J. Chem.*, 2017, **10**, S1913–S1922.
10 H. J. Tanudjaja, C. A. Hejase, V. V. Tarabara, A. G. Fane and J. W. Chew, Membrane-Based Separation for Oily Wastewater: A Practical Perspective, *Water Res.*, 2019, **156**, 347–365.
11 B. Li, B. Qi, Z. Guo, D. Wang and T. Jiao, Recent Developments in the Application of Membrane Separation Technology and Its Challenges in Oil-Water Separation: A Review, *Chemosphere*, 2023, **327**, 138528.
12 A. K. Kota, G. Kwon, W. Choi, J. M. Mabry and A. Tuteja, Hygro-Responsive Membranes for Effective Oil–Water Separation, *Nat. Commun.*, 2012, **3**(1), 1–8.
13 E. S. Dmitrieva, T. S. Anokhina, E. G. Novitsky, V. V. Volkov, A. V. Volkov and I. L. Borisov, Polymeric Membranes for Oil-Water Separation: A Review, *Polymers*, 2022, **14**(5), 980.
14 J. Huang, X. Ran, L. Sun, H. Bi and X. Wu, Recent Advances in Membrane Technologies Applied in Oil–Water Separation, *Discover Nano*, 2024, **19**(1), 1–21.
15 A. M. Lima, A. M. de Oliveira, T. G. de Sousa, A. C. Pereira, R. B. de Carvalho and W. A. Pinheiro, Filtration Membranes of Reduced Graphene Oxide for Dye Removal – Production and Characterization, *Desalin. Water Treat.*, 2022, **278**, 217–225.
16 A. Mansourizadeh and A. Javadi Azad, Preparation of Blend Polyethersulfone/Cellulose Acetate/Polyethylene Glycol Asymmetric Membranes for Oil-Water Separation, *J. Polym. Res.*, 2014, **21**(3), 375.
17 A. Hussain, M. Al-Yaari, A. Hussain and M. Al-Yaari, Development of Polymeric Membranes for Oil/Water Separation, *Membranes*, 2021, **11**(1), 42.
18 N. Hilal, O. O. Ogunbiyi, N. J. Miles and R. Nigmatullin, Methods Employed for Control of Fouling in MF and UF Membranes: A Comprehensive Review, *Sep. Sci. Technol.*, 2005, **40**(10), 1957–2005.
19 A. Mansourizadeh and A. Javadi Azad, Preparation of Blend Polyethersulfone/Cellulose Acetate/Polyethylene Glycol Asymmetric Membranes for Oil-Water Separation, *J. Polym. Res.*, 2014, **21**(3), 375.
20 R. K. Gupta, G. J. Dunderdale, M. W. England and A. Hozumi, Oil/Water Separation Techniques: A Review of Recent Progresses and Future Directions, *J. Mater. Chem. A*, 2017, **5**(31), 16025–16058.
21 W. Bai, J. Feng, C. Luo, P. Zhang, H. Wang, Y. Yang, Y. Zhao and H. Fan, A Comprehensive Review on Oxygen Transport Membranes: Development History, Current Status, and Future Directions, *Int. J. Hydrogen Energy*, 2021, **46**(73), 36257–36290.
22 M. Nau, N. Herzog, J. Schmidt, T. Meckel, A. Andrieu-Brunsen and M. Biesalski, Janus-Type Hybrid Paper Membranes, *Adv. Mater. Interfaces*, 2019, **6**(18), 1900892.
23 C. R. Reshmi, S. P. Sundaran, A. Juraij and S. Athiyanathil, Fabrication of Superhydrophobic Polycaprolactone/Beeswax Electrospun Membranes for High-Efficiency Oil/Water Separation, *RSC Adv.*, 2017, **7**(4), 2092–2102.
24 D. Zhu, C. Hu, R. Zhao, X. Tan, Y. Li, V. Mandić, Z. Shi and X. Zhang, Fabrication of Cerium Oxide Films with Thickness and Hydrophobicity Gradients, *Surf. Coat. Technol.*, 2022, **430**, 127985.
25 Z. Shi, Z. Zhang, W. Huang, H. Zeng, V. Mandić, X. Hu, L. Zhao and X. Zhang, Spontaneous Adsorption-Induced Salvinia-like Micropillars with High Adhesion, *Langmuir*, 2021, **37**(22), 6728–6735.
26 D. Zhu, X. Tan, L. Ji, Z. Shi and X. Zhang, Preparation of Transparent and Hydrophobic Cerium Oxide Films with Stable Mechanical Properties by Magnetron Sputtering, *Vacuum*, 2021, **184**, 109888.
27 D. Zhu, W. Liu, R. Zhao, Z. Shi, X. Tan, Z. Zhang, Y. Li, L. Ji and X. Zhang, Microscopic Insights into Hydrophobicity of Cerium Oxide: Effects of Crystal Orientation and Lattice Constant, *J. Mater. Sci. Technol.*, 2022, **109**, 20–29.
28 H. Zhu, S. Qiu, W. Jiang, D. Wu and C. Zhang, Evaluation of Electrospun Polyvinyl Chloride/Polystyrene Fibers as Sorbent Materials for Oil Spill Cleanup, *Environ. Sci. Technol.*, 2011, **45**(10), 4527–4531.
29 S. M. Rahman, S. Gautam, H. V. Tafreshi and B. Pourdeyhimi, The Role of 3D Electrostatic Field in Modeling the Electrospinning Process, *J. Appl. Phys.*, 2024, **135**(1), 014701.
30 M. Mathew, S. Paroly and S. Athiyanathil, Fabrication and Optimization of Highly Porous Electrospun PLA Fibers: A Comparative Study with Curcumin-Loaded Systems, *J. Polym. Res.*, 2025, **32**(4), 1–15.
31 C. R. Reshmi, S. P. Sundaran, A. Juraij and S. Athiyanathil, Fabrication of Superhydrophobic Polycaprolactone/Beeswax Electrospun Membranes for High-Efficiency Oil/Water Separation, *RSC Adv.*, 2017, **7**(4), 2092–2102.
32 C. Su, Y. Li, Y. Dai, F. Gao, K. Tang and H. Cao, Fabrication of Three-Dimensional Superhydrophobic Membranes with High Porosity *via* Simultaneous Electrospraying and Electrospinning, *Mater. Lett.*, 2016, **170**, 67–71.
33 Y. Cheng, X. Zhai, Y. Wu, C. Li, R. Zhang, C. Sun, W. Wang and H. Hou, Effects of Natural Wax Types on the Physicochemical Properties of Starch/Gelatin Edible Films Fabricated by Extrusion Blowing, *Food Chem.*, 2023, **401**, 134081.
34 C. R. Reshmi, S. P. Sundaran, K. Juraij and S. Athiyanathil, Fabrication of Superhydrophobic Polycaprolactone/Beeswax Electrospun Membranes for High-Efficiency Oil/Water Separation, *RSC Adv.*, 2017, **7**(4), 2092–2102.
35 C. R. Reshmi, S. P. Sundaran, K. Juraij and S. Athiyanathil, Fabrication of Superhydrophobic Polycaprolactone/Beeswax Electrospun Membranes for High-Efficiency Oil/Water Separation, *RSC Adv.*, 2017, **7**(4), 2092–2102.

36 K. Juraij, C. Chingakham, O. Manaf, P. Sagitha, V. Suni, V. Sajith and A. Sujith, Polyurethane/Multi-walled Carbon Nanotube Electrospun Composite Membrane for Oil/Water Separation, *J. Appl. Polym. Sci.*, 2022, **139**(19), 52117.

37 A. S. Niknejad, S. Bazgir, A. Sadeghzadeh and M. M. A. Shirazi, Evaluation of a Novel and Highly Hydrophobic Acrylonitrile-Butadiene-Styrene Membrane for Direct Contact Membrane Distillation: Electroblowing/Air-Assisted Electrospraying Techniques, *Desalination*, 2021, **500**, 114893.

38 S. Akkoyun and N. Öktem, Effect of Viscoelasticity in Polymer Nanofiber Electrospinning: Simulation Using FENE-CR Model, *Eng. Sci. Technol. Int. J.*, 2021, **24**(3), 620–630.

39 R. Kandi, P. M. Pandey, M. Majood and S. Mohanty, Fabrication and Characterization of Customized Tubular Scaffolds for Tracheal Tissue Engineering by Using Solvent Based 3D Printing on Predefined Template, *Rapid Prototyping J.*, 2021, **27**(2), 421–428.

40 J. J. Benítez, J. A. Heredia-Guerrero, S. Guzmán-Puyol, M. J. Barthel, E. Domínguez and A. Heredia, Polyhydroxyester Films Obtained by Non-Catalyzed Melt-Polycondensation of Natural Occurring Fatty Polyhydroxyacids, *Front. Mater.*, 2015, **2**, 153694.

41 H. Luo, H. Deng, Y. Zhu, H. Shi, C. Zhang and Y. Wang, High-Performance Polyurethane Elastomers with Mechano-Responsive Self-Reinforcing *via* Rigid-Flexible Segments Regulation, *Composites, Part B*, 2025, **297**, 112287.

42 H. Kuleyin, S. Budak, Ö. B. Yasan and R. Gümrük, Characterization of Thermal, Chemical, Mechanical, and Fatigue Behavior of 3D Printed ABS-Based Elastomeric Blends: ABS/EVA and ABS/TPU, *Polym. Test.*, 2025, **145**, 108763.

43 T. Mekonnen, P. Mussone, H. Khalil and D. Bressler, Progress in Bio-Based Plastics and Plasticizing Modifications, *J. Mater. Chem. A*, 2013, **1**(43), 13379–13398.

44 S. Hussain, R. Akhter and S. S. Maktedar, Advancements in Sustainable Food Packaging: From Eco-Friendly Materials to Innovative Technologies, *Sustainable Food Technol.*, 2024, **2**(5), 1297–1364.

45 Z. Shi, H. Zeng, Y. Yuan, N. Shi, L. Wen, H. Rong, D. Zhu, L. Hu, L. Ji, L. Zhao and X. Zhang, Constructing Superhydrophobicity by Self-Assembly of SiO2@Polydopamine Core-Shell Nanospheres with Robust Oil-Water Separation Efficiency and Anti-Corrosion Performance, *Adv. Funct. Mater.*, 2023, **33**(16), 2213042.

46 X. H. Shi, X. L. Li, Y. M. Li, Z. Li and D. Y. Wang, Flame-Retardant Strategy and Mechanism of Fiber Reinforced Polymeric Composite: A Review, *Composites, Part B*, 2022, **233**, 109663.

47 S. Li, J. Huang, Z. Chen, G. Chen and Y. Lai, A Review on Special Wettability Textiles: Theoretical Models, Fabrication Technologies and Multifunctional Applications, *J. Mater. Chem. A*, 2016, **5**(1), 31–55.

48 S. H. Kim, S. W. Na, N. E. Lee, Y. W. Nam and Y. H. Kim, Effect of Surface Roughness on the Adhesion Properties of Cu/Cr Films on Polyimide Substrate Treated by Inductively Coupled Oxygen Plasma, *Surf. Coat. Technol.*, 2005, **200**(7), 2072–2079.

49 X. Yang, Y. Chen, C. Zhang, G. Duan and S. Jiang, Electrospun Carbon Nanofibers and Their Reinforced Composites: Preparation, Modification, Applications, and Perspectives, *Composites, Part B*, 2023, **249**, 110386.

50 V. K. Balla, K. H. Kate, J. Satyavolu, P. Singh and J. G. D. Tadimeti, Additive Manufacturing of Natural Fiber Reinforced Polymer Composites: Processing and Prospects, *Composites, Part B*, 2019, **174**, 106956.

51 S. Mantripragada, S. Gbewonyo, D. Deng and L. Zhang, Oil Absorption Capability of Electrospun Carbon Nanofibrous Membranes Having Porous and Hollow Nanostructures, *Mater. Lett.*, 2020, **262**, 127069.

52 Z. Shi, C. Fang, J. Li, S. Bandaru, M. Liu, L. Zhao and X. Zhang, Multi-Dimensional Design of Slippery Liquid-Infused Coatings Empowering Long-Term Corrosion Protection for Sintered Nd-Fe-B Magnets in Harsh Environments, *Small*, 2025, **21**(22), 2500629.